Journal of the Chinese Society of Mechanical Engineers, Vol.47, No.3, pp 295~308 (2026)

Research on Structural Design Optimization and Damping Force Calculation of Single-cylinder Magnetorheological Damper

Na Lu*, Xiaoxiao Han* and Yan Liu**

Keywords: Single-cylinder magnetorheological damper; Structural design optimization; Damping force; Analysis for magnetic field

ABSTRACT

A single-cylinder magnetorheological damper was designed in this paper, and a single-cylinder magnetorheological damper damping force calculation method was proposed for the study of the damping characteristics of magnetorheological damper. Firstly, the damping force model of the single-cylinder magnetorheological damper was established; secondly, the magnetic domain model of the single-cylinder magnetorheological damper was established, and the magnetic field distribution was obtained by using the simulation software; finally, the relationship between the magnetic flux density of the core inlet and outlet and the coil current was obtained through experiments. The calculation results show the variation rule between the coil current and the damping force under different motion rates of the core, and are compared with the experimental data. The relationship between the damping force and the movement rate of the core was also shown when the clearance between the core and the inner wall of the cylinder cylinder varies.

INTRODUCTION

The unique properties of magnetorheological fluid make it widely used in the field of transmission, using this feature, the magnetorheological damper is manufactured with the advantages of light weight and low energy consumption; it has the characteristics of small size, controllable output damping force, and wide range of adjustment (Lijiang W et al., 2022. Jin H et al., 2022). Magnetorheological fluid damper is a promising device for automatic vibration control. The mechanical characteristics of magnetorheological damper are constrained by the magnetic field, frequency, amplitude and other factors, and its dynamical characteristics show a large nonlinearity (Huiting B et al., 2020).

At present, many scholars have carried out a lot of research on magnetorheological dampers. Hao X et al. (2020) used a single-tube inflatable magnetorheological body damper as a template to model the force exerted on its operation, and based on this, the structure of a single-cylinder inflatable magnetorheological damper was modeled and simulated; Tieying G et al. (2018) integrated the advantages of various types of magnetorheological mathematical models to establish an improved Bouc-Wen model, and the design and optimization of the structure was carried out ; Liejiang W et al. (2020) derived the formula for its output damping force by experimentally determining the relationship between the edge of the plug flow region and the motion rate of the plunger; Yuanzhi H (2019) investigated and analyzed the computational model of the damping force of a magnetorheological fluid damper based on the typical structure of the damper through the internal flow state and the motion condition of the piston; Chaoqun W et al. (2021) used a one-factor-variable method to analyze the influence of each magnetic circuit structural parameter on the magnetic field distribution of the damper, determine the optimized parameters of the magnetic circuit structure, and conduct damping characteristic tests to verify the reliability of its design; Munyaneza Olivier (2020) established a two-dimensional axisymmetric model of a hybrid magnetorheological damper to optimize the geometrical parameters and the damping force; Baozhen L et al. (2021) investigated that in the case of different non-uniform magnetic field distributions, magnetorheological liquid of magnetorheological fluids under different non-uniform magnetic field distributions.

The above established damping force model has the problems of inconvenient numerical treatment and complicated process, and the above studies on the damping force of magnetorheological fluid damper are mainly based on the analysis of the damping force under the magnetic field factor, and do not give the

Paper Received October, 2024. Revised June, 2025. Accepted July, 2025. Author for Correspondence: Xiaoxiao Han

**Professor, Wanjiang University of Technology, School of Mechanical Engineering, Maanshan in AnHui province, 243000, China.*

***Student, Wanjiang University of Technology, School of Mechanical Engineering, Maanshan in AnHui province, 243000, China.*

exact calculation method. This paper proposes a single cylinder magnetorheological damper damping force calculation method, the establishment of the damping force calculation model and the magnetic domain model, magnetic field simulation analysis, the relationship between the magnetic flux density and the coil current, as well as the core motion rate change, the coil damping force and the change rule of the coil current, and combined with the relevant experiments to obtain the relevant damping characteristics.

DAMPER STRUCTURE DESIGN AND PARAMETER OPTIMIZATION SIMULATION ANALYSIS

In the automotive industry, automotive dampers are usually called dampers (Duym S W R, 2000). Automotive dampers can be categorized into passive dampers, manually adjustable dampers and adaptive dampers according to the type of damping force change mechanism (Groves G W et al., 2002). The concept of adaptive dampers is limited to semi-active damping systems nowadays since the costs of active suspension systems are too high. In recent years, due to the research and development of smart materials, magnetorheological fluids have been used in semi-active automotive suspension systems.

Design of Integral Structure of Single-Cylinder Magnetorheological Damper

In consideration of the installation size of passenger car suspension and the clogging problem caused by magnetorheological fluid settling, the magnetorheological damper selects a single rod and single cylinder structure. In addition, in terms of increasing the effective working area of the damper (and the resulting field damping force), a two-stage coil control valve is used. The structural design of the magnetorheological fluid damper is shown in Fig.1.

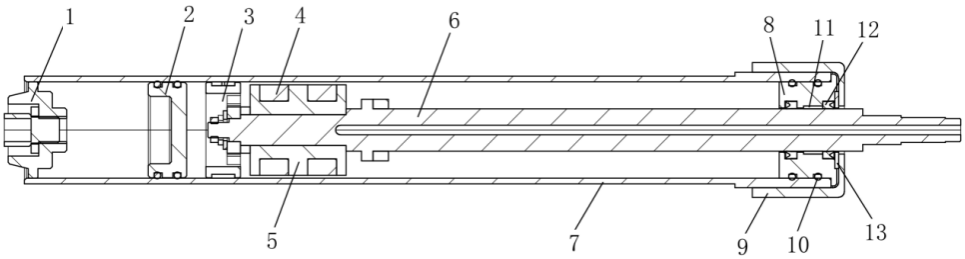

1-Filling valve; 2-Floating piston; 3-Piston; 4-Coil; 5-Core; 6-Piston rod; 7-Working cylinder; 8-Top seal; 9-Top cover; 10-Sealing ring; 11-Guidance ring; 12-Glyd ring; 13-Dust ring

Fig.1. Magnetorheological damper integral design structure

The main components of the magnetorheological damper include filling valve, floating piston, piston, coil, core, piston rod, working cylinder, top seal and top cover. Two stages of coils are wound in series and reversed on the core, and the wires are led out to the outside of the damper through a through-hole in the piston rod to connect with the control power supply. In the top seal part of the single-cylinder magnetorheological damper, in consideration of prolonging the service life of the seals, a two-stage U-ring seal and an additional dust ring are used, which can prevent external impurities and dust from entering the seals. In particular, a guide ring is mounted in the center of the top cover bore, which serves to prevent excessive interference with the piston rod and guiding of the piston rod during the up and down movement of the core. Lubricant is added when the piston rod is first installed with the U-ring and guide ring, and is not required subsequently. The magnetorheological fluid acts as a lubricant even if there is a small leakage. In addition, a protective coating is applied to the outside of the coil for protection.

The single-cylinder magnetorheological damper differs from a conventional damper in its principle of operation. In a conventional damper, hydraulic fluid is passed through a damping channel, causing the pressure in the upper and lower chambers to change, thereby creating a damping force to effectively regulate vibration. Magnetorheological damper is in the piston up and down movement, through the damping channel flow through the magnetorheological fluid, part of the magnetorheological fluid due to its characteristics in the working process will produce viscous damping phenomenon. When the excitation current acts between the piston and the working chamber, the magnetic field forms a shear stress, which generates a certain pressure between the upper and lower working chambers, thus producing an adjustable damping force. In addition, during the filling process with an inert gas (e.g. nitrogen), the filling valve generates a damping force at the same time to counteract the pressure change in the working chamber.

Selection and Calculation of Main Structural Parameters

The main structural parameters of the single-cylinder magnetorheological damper are designed and calculated (QC/T 491-1999. Feng Z et al., 2022).

The preliminary determined structural dimension parameters are shown in Table 1.

Table 1. Preliminary structural dimension parameters

Name	Parameter
Work cylinder inner diameter D(mm)	50
Work cylinder outer diameter D_1(mm)	56.5
Work cylinder length L_1(mm)	420
Damping clearance h(mm)	1.2
Core diameter D_2(mm)	47.6
Piston rod diameter d(mm)	12.5
Effective working length of piston rod l_s(mm)	6
Magnetorheological fluid viscosity μ	0.6

Magnetorheological Fluid Damper Magnetic Circuit

In a single-cylinder MR damper, the effect of magnetic field on the performance is particularly significant. Therefore, the magnetic circuit design is critical in the structural design, and one of the key components is the excitation coil. Many factors of the excitation coil directly affect the output damping force of the damper.

Magnetic Circuit Design

The magnetic circuit is mainly magnetically conductive is ferromagnetic material, other substances still have the ability to conduct magnetism, but relative to ferromagnetic material, only a small portion of the magnetic flux will pass through the path outside the iron core to constitute a leakage magnetic circuit, which is generally negligible in theory (Gang C et al., 2008).

The following issues need to be noted in the design of the magnetic circuit:

(1) Selection of magnetically conductive materials. The general magnetic conductivity material is selected as high as possible to meet the magnetic induction strength of the working area, which can reduce the loss of the core part of the magnetic circuit. In this paper, the material of the iron core is selected DT4 electric pure iron.

(2) Damping clearance. As far as possible to reduce the damping clearance, the damping clearance size of 1.2 in this paper.

(3) Excitation coil. The excitation coil selects copper wire, the excitation coil as far as possible to select a larger diameter of high-quality enameled wire, reducing the coil resistance and heat generation. In this paper, the choice of polyester imide (QZY) enameled wire, resistant to 180 high temperature, copper core diameter of 0.35, the maximum outer diameter of the enameled wire 0.4. In the magnetic circuit to determine the size of the good, you need to consider the number of turns of the coil, the number of turns selected 200. In order to prevent coil overheating loss, the current size of the coil to control in the 0-2A.

As shown in Fig.2, the two-stage coil magnetic circuit structure schematic diagram, the core is equipped with internal holes with the piston rod interplay, there are step-through holes used to lead to the enameled wire. Taken together, the main structural parameters of the magnetic circuit part are shown in Table 2.

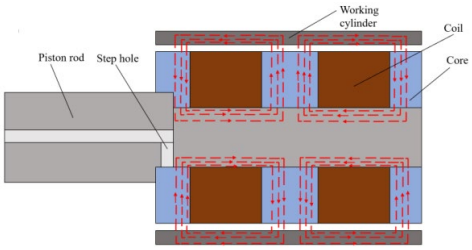

Fig.2. Structure diagram of the actual two-coil magnetic circuit

Table 2. Magnetorheological damper magnetic circuit part of the structural parameters

Name	Parameter
Coil groove depth b（mm）	9
Core length L（mm）	50
Core left side length l_1（mm）	6
Length of coil slot l_2（mm）	13
Core middle length l_3（mm）	12
Coil current I（A）	0-2
Number of turns of coil at each stage N（turns）	200

Simulation Study of Magnetic Field of Magnetic Circuit

The single-cylinder MR damper is equipped to adjust the size and range of the output damping force by modifying the magnetic field strength of the coil set inside the MR damper.The damping force of the MR damper can be carried out by adjusting the size of the electric current.To determine the relationship between the current of the coil and the flux density of the channel, finite-element computational analysis is carried out on the magnetic circuit portion, and the magnetic field distribution inside the two-stage magnetic circuit is analyzed in the presence of different current sizes.

The magnetic domain model of the flow channel is established based on the designed single-cylinder MR damper structure, as shown in Fig.3. Since the model only simulates the magnetic field distribution, parts unrelated to the magnetic field simulation are omitted, and only the cylinder, the core, the coil, and the magnetorheological fluid inside the damping channel are retained.

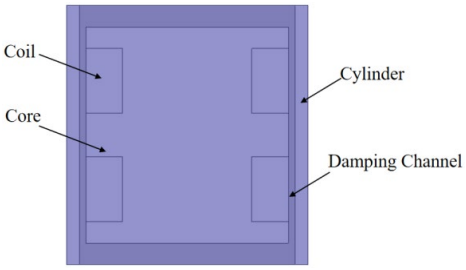

Fig.3. Magnetic field model

(1) Establish the magnetic circuit magnetic field analysis model

Magnetic field analysis model includes the construction of geometric models, define the material properties and boundary conditions, set the excitation conditions, the division of the unit mesh and solve the analysis.

1) Magnetic circuit model

Create a new project and select the Magnetostatic solver for solving. Select the static magnetic field for the finite element analysis of the magnetic circuit, and according to the structural parameters, build a geometric model as shown in Fig.4.

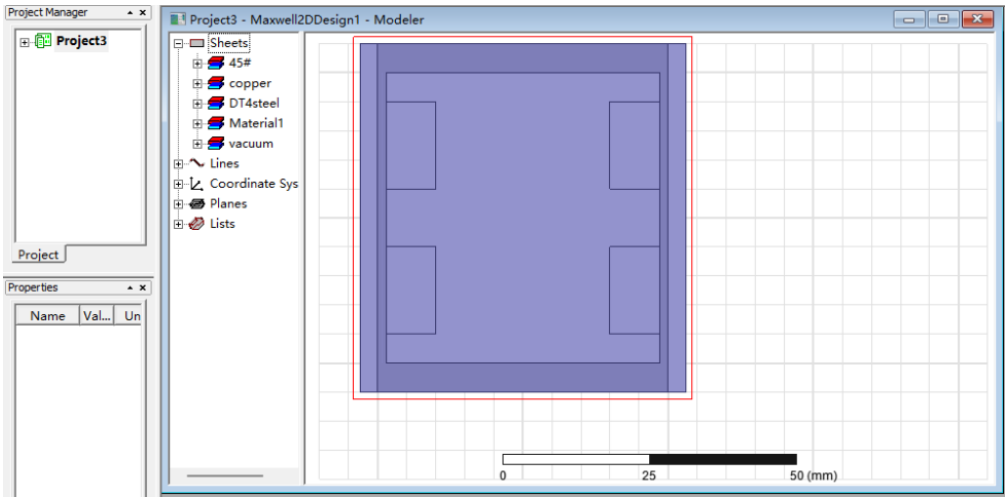

Fig.4. Magnetic circuit geometry model

2) Define material properties

The material properties are defined before the magnetic field analysis. Table 3 shows the B-H values of the magnetorheological fluid, the material of the working cylinder (45# steel), and the material of the core (DT4 type electrical pure iron), respectively. The material chosen for the coil is copper; the rest is defined as vacuum.

Table 3. B-H values of materials

Magnetorheological fluid		45# steel		DT4 type electrical pure iron	
$B(T)$	$H(KA/m)$	$B(T)$	$H(KA/m)$	$B(T)$	$H(KA/m)$
0	0	0	0	0	0
0.0376	2	0.2	0.4	0.2	21.2
0.1354	14	0.5	0.65	0.4	42
0.2333	29	0.75	0.9	0.6	63.2
0.3203	46	1	1.5	0.8	84.8
0.5268	92	1.25	2.36	1	104
0.7008	147	1.5	4	1.1	120
0.8204	196	1.6	5.4	1.2	135
0.8965	234	1.7	7.8	1.4	220
0.9183	245	1.8	11.2	1.5	480
0.9617	271	1.9	16	1.6	1600

3) Define boundary conditions and excitation
Outside the structural model needs to set a boundary condition, set the solution domain region and then define the current excitation, the number of turns of the coil is 200, the product of the number of turns and the magnitude of the added current is the value of the multilevel coil current, and four sets of data are set up here, respectively, 100A, 200A, 300A, and 400A.

4) Module selection and meshing
Mesh division is performed. The length of the coil part of the module mesh is set to 3; the length of the core material module mesh is set to 6; the length of the module mesh at the clearance of the damping channel is set to 2; the length of the module mesh in the cylinder cylinder part is set to 6; and the rest of the part is set to 10, as shown in Fig.5.

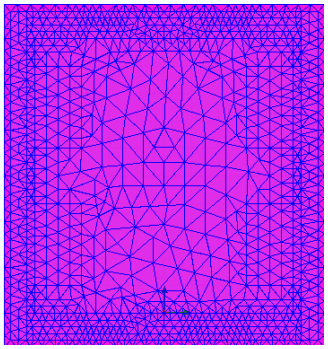

Fig.5. Magnetic circuit meshing

5) Solve
After adding the solution option, the model can be verified, and when the model has no error report, the finite element model analysis and solution step is carried out. After the completion of the solution, the conclusion of the analysis of the data after the conclusion of the analysis, and output the desired data and information.

(2) Magnetic circuit saturation analysis

Magnetic flux in the magnetic circuit is equivalent anywhere, the magnetic induction strength of the magnetically conductive medium has a saturation characteristic, will not increase indefinitely, the value of which is the product of the flux area and its saturation magnetic induction strength. Magnetic circuit in the magnetic flux through the ability of the smallest part of the flux is the smallest part of the flux, its smallest part of the first into the magnetic saturation state, the magnetic flux of the full magnetic circuit is also in a saturated state, thus having an impact on the flux capacity of the full magnetic circuit. When the applied magnetic field continues to increase, the magnetic field strength of the magnetorheological fluid will not increase, thus restricting the maximum output power of the magnetorheological fluid and the growth of adjustable damping force. Magnetic saturation is investigated when carrying out magnetic circuit design to avoid premature magnetic saturation, thus increasing the magnetic flux of the magnetorheological fluid and improving the working capability of the magnetorheological fluid. The results of the magnetic saturation analysis of the magnetic circuit are summarized in Table 4.

Table 4. Magnetic saturation analysis results of magnetic circuit

	Iron core area R_{m11}	Iron core area R_{m21}	Iron core area R_{m23}	Damping channel clearance area R_{m01}	Cylinder area R_{m31}
Magnetic flux area formula	$\pi = \left[\frac{D_4^2}{4} - \frac{d^2}{4}\right]$	$\pi D_2 l_1$	$\pi D_2 l_3$	$\pi D_2 l_1$	$\pi\delta(\delta + 2h + D_2)$
Magnetic flux area value(mm^2)	565.1	896.8	1793.6	896.8	543.4
Magnetic saturation induced intensity $B/(T)$	1.5	1.5	1.5	0.6	1.5
Maximum magnetic flux $\Phi/(\mathrm{Wb})$	0.000848	0.00135	0.00269	0.000538	0.000815
Magnetic saturation order	III	IV	V	I	II

Analyzing the values in Table 4, the damping channel clearance reaches the magnetic saturation state first, and the area that appears magnetic saturation state immediately after is at the cylinder barrel area. In the case of the same magnetic flux, the small area reaches the saturation state first, and the core region, the iron core region, and the iron core region reach the magnetic saturation state successively. Therefore, only the damping channel clearance region and the core region are analyzed for the magnetic saturation state, and the structural parameters of the single-cylinder magnetorheological damper are optimized to maximize the magnetic saturation of these two regions.

In the simulation software, after establishing the magnetic circuit structure and defining the material properties and boundary conditions, the electromagnetic field distribution of this magnetic

domain model is analyzed by inputting the excitation currents of 0.5, 1, 1.5, and 2. The magnetic induction intensity of the magnetic circuit is shown as a cloud graph in Fig.6, and the intensity of the magnetic induction is shown as the magnetic induction intensity under different excitations in Fig.7.

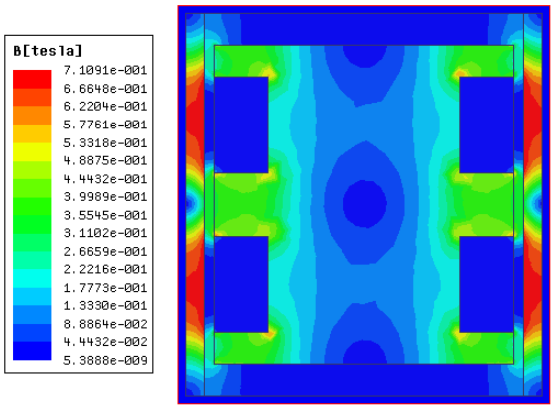

Fig.6. Magnetic induction intensity cloud graph

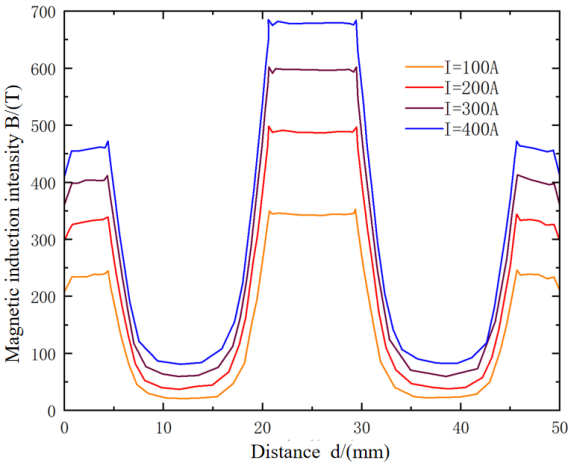

Fig.7. Magnetic induction intensity under four current values

From Fig.6 and Fig.7, it can be seen that the saturation magnetic induction intensity of each magnetic circuit is within the maximum range of its material saturation magnetic induction intensity, and the order of the five regions reaching the magnetic saturation state in turn matches the results of the theoretical calculation and analysis, which indicates that the current design calculations are in line with the design requirements.

Optimization of magnetorheological fluid damper parameters

The magnitude of the magnetic field in the damping channel is related to the structural parameters of the magnetic circuit, and with the change of the structural parameters of the magnetic circuit, the magnetic field will change accordingly. To improve the performance of single-cylinder magnetorheological damper effectively, it makes sense to optimize its structural parameters.

Multi-objective genetic algorithm

In this paper, Multi-objective Genetic Algorithm (MOGA) is used to optimize the structural parameters (Li Q, 2020).

Parameter settings have a critical impact on the operational structure of the MOGA , including population size, crossover probability, mutation probability, and number of evolutionary generations. The proper configuration of parameters is carried out before starting the MOGA .

Design variables

In consideration of the magnetic circuit design and performance characteristics of the MRF damper, the parameters damping channel effective area length l_1, damping channel non-effective area length l_2, damping channel clearance h, and the coil groove depth b, core coil radius difference b_1, cylinder cylinder thickness δ, and piston rod radius r, which are the seven structural dimensions, are used as design variables, as shown in Fig.8.

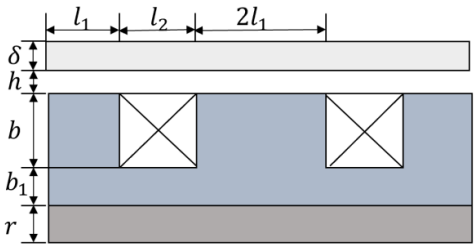

Fig.8.Structural optimization of dimensional parameters

The optimized range of structural parameters is defined after comprehensive consideration as shown in Table 5.

Table 5. Optimization variables

Variable name	Design initial value/mm	Optimization range /mm
Damping channel clearance h	1.2	0.5-1.5
Damping channel effective area length l_1	6	5-8
Damping channel non-effective area length l_2	13	10-18

Coil slot depth b	9	5-10
Core coil radius difference b_1	8.55	5-10
Cylinder barrel thickness δ	3.25	2.5-4
Piston rod radius r	6.25	5.5-7.5

Objective function

The performance evaluation indexes of the single-cylinder MR damper as a damping force adjustable damper mainly include the maximum damping force, the maximum damping adjustable coefficient, and the magnetic circuit response time (Dong K et al., 2023. Chunyuan L et al., 2023).

The maximum damping force can be provided when the single-cylinder MR damper reaches the magnetic flux saturation state and the The multi-objective optimization seeks to minimize the objective value, so $-F$ can be set as the objective function, then, solving the maximum damping force problem becomes solving the minimum value of $-F$. According to the basic formula of the damping force in different operating modes of the MR damper. The objective function$f_1$can be determined.

$$f_1 = -\left[\frac{12\mu(4l_1+2l_2)A_p^2}{\pi D_1 h^3}v + \frac{12l_1\tau_y A_p}{h}sgn(v)\right] \quad (1)$$

Where, $sgn(v) = \begin{cases} 1, & v>0 \\ -1, & v<0 \end{cases}$;

A_pPiston effective area;

$\tau_y$is shear yield strength.

From equation (1), f_1 can be viewed as consisting of two components, the liquid viscous damping force F_μ and the Coulomb damping force F_τ. $F_\mu$is related to the speed of motion of the piston, while $F_\tau$is related to the magnetic field.

$$F_\mu = \frac{12\mu(4l_1+2l_2)A_p^2}{\pi D_1 h^3}v, F_\tau = \frac{12l_1\tau_y A_p}{h}sgn(v)$$

The maximum power adjustable coefficient can be expressed as the ratio of to as in equation (2).

$$\beta = \frac{F_\tau}{F_\mu} = \frac{\pi D_1 l_1 \tau_y h^2}{(4l_1+2l_2)\mu A_p v} = \frac{(b+b_1+r+h+\delta)l_1\tau_y h^2}{\mu(2l_1+l_2)[(b+b_1+r+h+\delta)^2-r^2]v} \quad (2)$$

Therefore, the objective function $-\beta$ can be determined by setting the optimization objective function to f_2, as in equation (3).

$$f_2 = -\frac{(b+b_1+r+h+\delta)l_1\tau_y h^2}{\mu(2l_1+l_2)\left[(b+b_1+r+h+\delta)^2-r^2\right]v} \quad (3)$$

Optimization objectives

When the response time of the magnetic circuit is short, the vibration damping effect of the single-cylinder MR damper is better. When the response time of the magnetic circuit does not exceed a certain interval, the operating characteristics of the damper are well satisfied, so the effect of the response time of the magnetic circuit is not taken into account when performing the structural optimization.

The objective function $f_1 = -F$ of maximum damping force and the objective function $f_2 = -\beta$ of maximum damping adjustable coefficient are determined. The motion speed of the piston is 0.52 m/s, and the viscosity coefficient of the MRF is determined to be $\mu = 0.6$Pa•s, and the shear stress is $\tau_y = 45$ kPa, which can be determined as the optimization objective.

$$700N \le FN_{max} \le 9800N; 1.5 \le \beta \le 5$$

Analysis of optimization results

Before performing the optimization calculation, the algorithm parameters need to be set, the sample capacity is set to 100, and the crossover probability and variance probability are set to 0.65 and 0.02, respectively.

In the process of running the algorithm, the individuals are updated every time they evolve until the end of the algorithm run, and based on the results of the run, the Pareto solution set is plotted, as in Fig.9.

Since the initial values of the program are randomized for each run, some of the optimal solutions are shown in Table 6.

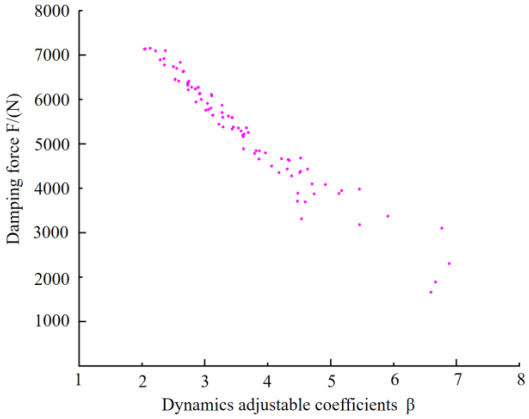

Fig.9. Pareto solution set for multi-objective optimization

As can be seen from Fig.9, under certain constraints, the relationship between the two objective functions elevated is contradictory, and when one

objective function is elevated, the other objective function is reduced. That is, the smaller the damping force is, the larger the power adjustable coefficient is, while the larger the damping force is, the smaller the power adjustable coefficient is.

In this optimization, the solution with larger damping force is considered to meet the requirement when the power adjustable coefficient is 2.2. From the results of the program, a set of optimal solutions is selected from the Pareto solution set of multi-objective optimization in Fig.9, and the design parameters before and after optimization are combined with the actual ones as shown in Table 7.

Table 6. Partial Pareto optimal solutions set

r /(mm)	b_1/(mm)	b /(mm)	h /(mm)	δ /(mm)	l_1/(mm)	l_2/(mm)
6.311606871	9.732727407	9.129375759	1.46422771	3.35898735	7.725428826	16.02686701
6.331396281	9.841365835	8.628217095	1.42602006	3.39651123	7.854316655	16.81206134
6.014289081	9.683670273	6.590502692	1.49081218	3.481903558	6.037894608	15.45465174
6.561658376	9.449577032	9.473471732	1.48136652	3.041496408	7.463979994	15.71052236
5.623027014	9.757563358	9.577696964	1.49372412	3.586164578	7.799347776	16.93286166
6.725269066	9.91115927	9.814977491	1.47561981	3.150965145	5.909217948	17.82710228
6.680912508	9.183951187	9.62945117	1.47260273	3.693990802	7.532278371	16.21824594
6.635866352	9.688993048	9.319507373	1.4897588	3.617707572	7.672536742	17.07734583
6.806371044	9.396335931	9.864051103	1.49999939	3.599993947	7.890984673	15.70062222

Table 7. Structural parameters before and after optimization

Structural parameter	Value before optimization	Value after optimization
h /(mm)	1.2	1.5
l_1/(mm)	6	5
l_2/(mm)	13	15
b /(mm)	9	8.5
b_1/(mm)	8.55	9
δ /(mm)	3.25	3
r /(mm)	6.25	6

The structural parameters before and after optimization are substituted into the optimization objective equation (1) and (3), and the pre-optimization objective function can be obtained, which are all in the optimization target range. After the optimization of the objective function, also in the optimization of the target range, after the optimization of the maximum damping force is smaller than the pre-optimization of the maximum damping force, but the maximum damping adjustable coefficient increased, within a reasonable range, the larger the maximum damping adjustable coefficient, can provide a more flexible, accurate, adaptable and energy-saving and environmentally friendly vibration control solutions, so as to play an important role in a variety of engineering applications.

The finalized overall structural dimensions of the damper are shown in Table 9.

Table 9. Finalized structural parameters of single-cylinder MR damper

Parameter	Value
D /(mm)	50
D_1/(mm)	56
D_2/(mm)	47
D_4/(mm)	30
L_1/(mm)	420
L /(mm)	50

SINGLE-CYLINDER MAGNETORHEOLOGICAL DAMPER DAMPING FORCE MODLE

The MRF exhibits non-Newtonian fluid flow characteristics under the action of an applied magnetic field, and a Bingham fluid model is used to study the MRF flow characteristics (Hongliang Z et al., 2021). This fluid model can be expressed by equation (4).

$$\begin{cases} \tau = \tau_Y + \mu \frac{du}{dy}, & \tau > \tau_Y \\ \tau = \tau_Y, & \tau \le \tau_Y \end{cases} \tag{4}$$

where, τ_Y- shear yield strength of MRF (MPa);
μ -viscosity coefficient of the MRF (Pa•s);
u -velocity along the flow direction (m/s).
While the MRF flows inside the damper cylinder

barrel, it can be assumed that the MRF only has the motion velocity along the axial direction of the damper, while the velocity along the circumferential and radial directions is negligible, and the flow model of the MRF inside the damper can be equivalently regarded as a two-dimensional flow field model as shown in Fig.10 (Decai L et al., 2020. Hua M et al., 2021).

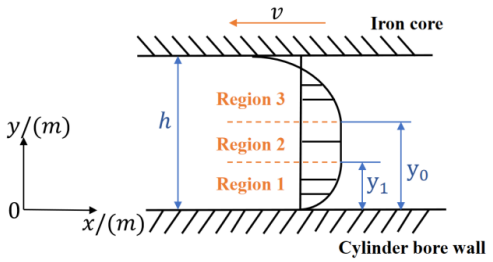

Fig.10. Fluid velocity distribution in the flow channel of a single-cylinder MR damper.

Since the MRF has non-Newtonian fluid flow characteristics, there is a "nuclear zone" within the flow layer. As the fluid interlayer shear strength within the nuclear zone is less than the critical shear strength, the fluids within the nuclear zone have the same flow velocity. With the flow channel wall adhesion of the fluid velocity and the velocity of the inner wall of the channel is the same, the inner wall of the flow channel and the nuclear zone between the fluid layer, the shear strength is higher than the shear yield strength, so it shows laminar flow characteristics.

To summarize, the fluid in the flow channel can be divided into three flow regions, i.e., region 1, region 2, and region 3, where region 2 represents the nuclear region and region 1 and region 3 represent the laminar flow region. From the flow velocity distribution, the boundary conditions within the different flow regions can be derived. The coordinate system in Figure12, the x-axis represents the direction of the core motion, and the y-axis represents the radial direction of the damper, then the boundary conditions in the different regions can be expressed as.

Region 1: $0 \le y \le y_1, u_1|_{y=0} = 0, \frac{du_1}{dy}|_{y=0} = 0$

Region 2: $y_1 \le y \le y_0, \frac{du_2}{dy} = 0$

Region 3: $y_0 \le y \le h, u_3|_{y=h} = -v, \frac{du_3}{dy}|_{y=h} = 0$

By integrating the control equations for the fluid flow as in equation (5).

$$\frac{\partial r}{\partial x} = \mu \frac{\partial^2 u}{\partial y^2} \tag{5}$$

Combined with the above boundary conditions for the different regions, the flow velocity distribution functions for the three different regions can be derived.

Region 1: $u_1 = \frac{1}{2\mu}\frac{dp}{dx} y(y-2)y_1$

Region 2: $u_2 = u_0$

Region 3:

$$u_3 = \frac{1}{2\mu}\frac{dp}{dx} y^2 - \frac{1}{\mu}\frac{dp}{dx} y_0 y + \frac{1}{2\mu}\frac{dp}{dx}(2y_0 - h)h - v$$

Since the flow velocities in the nuclear region are equal everywhere, the following equational relationship can be obtained.

$$u_1|_{y=y_1} = u_0 = u_3|_{y=y_0}$$

Solve it.

$$y_0 = h - \sqrt{y_1^2 - \frac{2\mu v}{\frac{dp}{dx}}}$$

In individual regions, the flow rate of the liquid can be expressed by equation (6).

$$Q = -\frac{\pi D_2}{6\mu}\frac{dp}{dx}\left[3hy_1^2 - y_1^3 - (y_1^2 + \frac{4\mu v}{\frac{dp}{dx}})\sqrt{y_1^2 - \frac{2\mu v}{\frac{dp}{dx}}}\right] - \pi D_2 v\sqrt{y_1^2 - \frac{2\mu v}{\frac{dp}{dx}}} \tag{6}$$

It follows from the equilibrium of forces on a non-Newtonian fluid in the nuclear region.

$$\frac{\Delta p}{L} = \frac{2\tau_Y}{y_0 - y_1} = \frac{2\tau_Y}{h - y_1 - \sqrt{y_1^2 - \frac{2\mu v}{\frac{dp}{dx}}}}$$

The solve is as in equation (7).

$$y_1 = \frac{1}{2}(h - \frac{2L\tau_Y}{\Delta p}) + \frac{\mu v}{(h - \frac{2L\tau_Y}{\Delta p})\frac{dp}{dx}} \tag{7}$$

With linearization of the non-Newtonian fluid pressure gradient, the fluid flow rate in the flow channel can be expressed as equation (8).

$$Q = \frac{\pi D_2}{3}\left\{\begin{array}{l}\frac{\Delta p}{\mu L}(h + \frac{L\tau_Y}{\Delta p})\left[\frac{h}{2} - \frac{L\tau_Y}{\Delta p} - \frac{\mu v L}{\Delta p(h - \frac{2L\tau_Y}{\Delta p})}\right]^2 \\ -v\left[\frac{h}{2} - \frac{L\tau_Y}{\Delta p} + \frac{\mu v L}{\Delta p(h - \frac{2L\tau_Y}{\Delta p})}\right]\end{array}\right\} \tag{8}$$

Based on the maximum cross-sectional area of the core, the fluid flow in the flow path can also be expressed as equation (9).

$$Q = Av = \frac{\pi D_2^2}{4} v \tag{9}$$

Δp in equation (11) may be represented by equation (10).

$$\Delta p = \frac{F}{A} = \frac{4F}{\pi D_2^2} \tag{10}$$

From equations (6)-(9), the damping force is implicitly modeled as in equation (11).

$$\frac{3}{4} D_2 v = \frac{4F}{\pi D_2^2 \mu L}(h + \frac{\pi D_2^2 L\tau_Y}{4F})(\frac{h}{2} - \frac{\pi D_2^2 L\tau_Y}{4F} - \frac{\pi D_2^2 \mu v L}{4Fh - 2\pi D_2^2 L\tau_Y})^2 - v(\frac{h}{2} - \frac{\pi D_2^2 L\tau_Y}{4F} + \frac{\pi D_2^2 \mu v L}{4Fh - 2\pi D_2^2 L\tau_Y}) \tag{11}$$

The output damping force can be expressed as equation (12).

$$F = 16D_2 L^6 \tau_Y^5 \pi - 3\pi D_2^2 v h^2 \mu - 12L^2 \pi D_2^2 v \mu \tau_Y^2 + D_2 L h^5 \pi + 16D_2 L^3 h^3 \tau_Y^2 \pi - 8D_2 L^4 h^2 \tau_Y^3 \pi +$$

$$12L\pi D_2^2 vh\mu\tau_Y - 16D_2L^4h\tau_Y^4\pi - 2D_2h^3\mu v\pi - 7D_2L^2h^4\tau_Y\pi - 4D_2Lh\mu^2v^2\pi - 4D_2L^2h^3\mu v\pi + 4D_2L^3h\mu^2v^2\pi + 8D_2L^2\mu^2v^2\tau_Y\pi + 4D_2L^4\mu^2v^2\tau_Y\pi + 16D_2L^3\mu v\tau_Y^3\pi - 16D_2L^5\mu v\tau_Y^3\pi + 12D_2Lh^2\mu v\tau_Y\pi - 24D_2L^2h\mu v\tau_Y^2\pi + 12D_2L^3h^2\mu v\tau_Y\pi \quad (12)$$

From equation (12), it is observed that when the MRF in the damping channel is in the flow state, the output damping force of the MR damper is related to the core diameter, the core speed, the shear yield strength of the MRF, the viscosity coefficient of the MRF, the velocity of the MRF along the flow direction, the length of the damping channel, and the clearance of the damping channel. When the core diameter, the damping channel length, and the core motion velocity increase, the damping force increases; and when the damping channel clearance decreases, the damping force increases. Therefore, when the MRF in the damping channel is in the flow state, the output damping force of the MR damper is directly proportional to the core diameter, core speed, and damping channel length, and inversely proportional to the damping channel clearance.

SINGLE-CYLINDER MAGNETORHEOLOGICAL DAMPER PERFORMANCE TEST

Based on the optimization of the structural design, the feasibility of the design is verified through simulation analysis, and the relevant parameters of the damper are determined. Modeling and analysis of the damping force, and mechanical design and drafting processing, assembly test, as shown in Fig.11 for the single-cylinder MR damper prototype. Finally, the damper damping force test bench is built and the damper device is debugged, and the experimental test is analyzed after the test is feasible.

The shear yield strength of the MRF depends on the applied magnetic flux density, and the damping force of the MR damper can be adjusted by adjusting the magnitude of the current, therefore, it is necessary to determine the current of the coil and the flux density of the channel as well as the relationship between the flux density and the shear yield strength of the MRF. The latter can be obtained by well-established experimental means and the former by electromagnetic finite element simulation.

Fig. 11. Single-cylinder MR damper

Magnetorheological damper test programs

The optimized single-cylinder magnetorheological damper is investigated experimentally and its output damping force is tested at different currents and speeds to verify the reasonableness of the design method. At the same time, the performance test of the developed MR damper is carried out to provide experimental reference and relevant experience for the subsequent development of MR damper.

Test Machine

The MR damper damping force test machine is a customized set of test bench for vibration testing. The test bench is shown in Figure 14, the upper end of the magnetorheological damper is fixed on the test bench through the mounting assembly, which contains a force transducer for measuring the damping force. The internal wires of the damper are connected to the external controller through the over crossing holes in the mounting assembly, and the mounting assembly is fixed to the upper slide of the test bench frame, which can be controlled in accordance with the control The slider can slide along the rail at a specified speed according to the control.

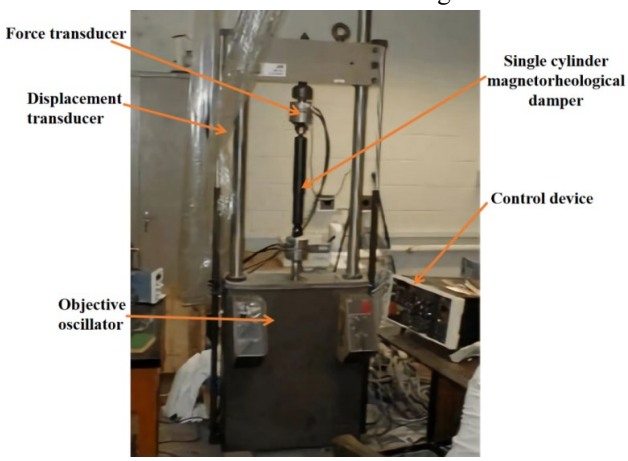

Fig.12. Single-cylinder MR damper damping force test bench

Test conditions

According to the relevant test guidelines (QC/T545-1999), the single-cylinder magnetorheological damper damping force test bench in Fig.12 is employed to conduct the relevant tests on the single-cylinder magnetorheological damper, and the specific test conditions are set as follows:

(1) The single-cylinder magnetorheological damper was stored at room temperature for not less than 6 hours before the test;
(2) The test amplitude of the damper is ±50mm (stroke 100mm), simple harmonic motion;
(3) Test initial position setting: set roughly in the middle part of the MR damper stroke;
(4) Test direction: Lead hammer direction;
(5) Excitation current range: 0-3A, test currents are: 0A, 0.5A, 1.0A, 1.5A, 2.0A, 2.5A, 3.0A;
(6) Test speed: 0.5 m/s, 1.0 m/s, 1.5 m/s, 2.0 m/s.

Test method

Design the upper and lower fixtures of the single-cylinder magnetorheological damper damping force test bench according to the structural dimensions of the homemade single-cylinder MR damper, install and fix the pre-tested single-cylinder magnetorheological damper on the test bench, and after that connect the exposed wires of the single-cylinder magnetorheological damper with the current control device, and utilize the input-output digital signaling device on the test bench to set up the pre-tested values of each speed, and adjust the The excitation current is adjusted so that it can be increased to the maximum in a small range and then reduced to the minimum, and then the test bench is activated to measure the damping force under different currents and different speeds and displacements by using the working device of the single-cylinder MR damper damping force test bench to obtain the required test data.

Test results and data analysis

According to the magnetorheological damper structure, the number of turns of the two-stage coil on the core is 200 turns, and changing the different coil currents, the magnetic flux density values at the inlet and outlet of the runner can be obtained, and the results are shown in Fig.13. It is easy to see from the correspondence between the magnetic flux density and the current that there is a proportional change between the magnetic flux density at the mouth of the runner and the current, and through straight-line fitting, it can be approximated to get the magnetic flux density at the mouth of the runner and the coil current. expression as equation (13).

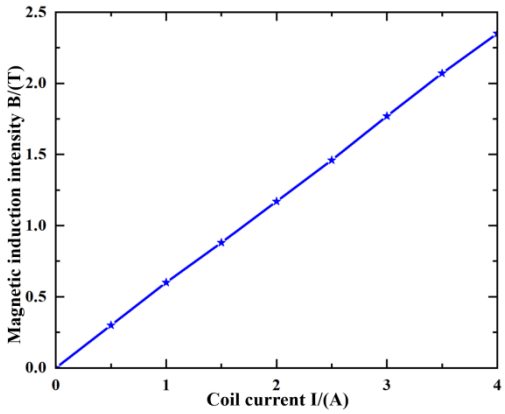

Fig.13. Flow channel inlet and outlet flux density versus coil current

The magnetorheological fluid used in this paper has been tested for its performance and the relationship between the shear yield strength τ_Y and the magnetic flux density B is shown in equation (14).

$$\tau_Y = -79.64B^3 + 111.4B^2 + 16.03B + 0.1251(kPa) \quad (14)$$

The relationship between the magnetorheological fluid shear yield strength and the coil current can be obtained from equations (13) and (14) as in equation (15).

$$\tau_Y = -16.15I^3 + 38.45I^2 + 9.42I + 0.1251(\text{kPa}) \quad (15)$$

To verify the results obtained from the damping force calculation method proposed in this paper are correct, the real damping force of the damper will be obtained from the damping force test bench as the comparison data.

The values of damping force versus current at different core speeds are obtained from the test, as shown in Fig.14, which demonstrates the relationship between damping force and coil current at different core speeds. From the results, it can be clearly seen that with the increase of coil current, the damping force of the damper shows the change rule of increasing first and then decreasing due to the flow properties of the magnetorheological fluid, and the shear yield strength of the magnetorheological fluid also becomes the change rule of increasing first and then decreasing only when the coil current is increased, and the results

show that the shear yield performance of the magnetorheological fluid has great influence. It should also be noted that when there is no current in the coil, the damping force increases with the increase of the core speed, but when the coil is energized with current, although the damping force also increases with the increase of the core speed, the magnitude of change is very small. The values of the damping force measured by the experiment are also given in the results, and the experimental results are able to match well with the calculated results.

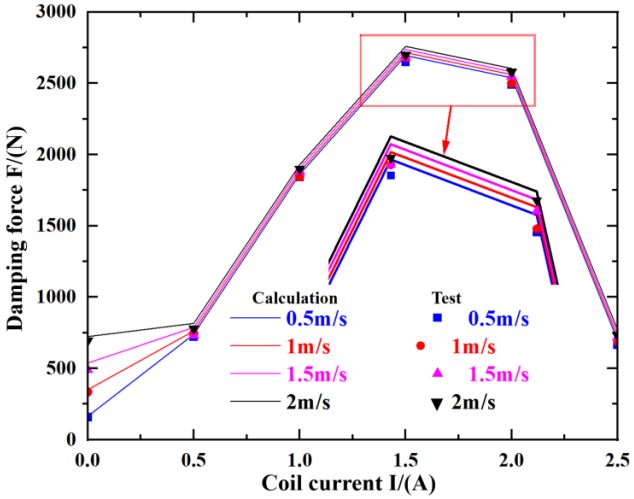

Fig.14. Relationship between damping force and coil current for different core speeds

The test also measured the values of the core speed and damping force when the clearance between the core and the cylinder cylinder varies, and the values of the core speed and damping force when the damping clearance is 1 mm, 1.5 mm and 2 mm were tested respectively. Fig.15 gives the change rule of the core speed and damping force when the core and cylinder cylinder clearance changes. From the results, it can be seen that the smaller the clearance, the larger the damping force, this is because, the smaller the clearance, the smaller the flow of magnetorheological fluid through the flow channel per unit of time, the magnetorheological fluid that fails to flow out in time produces a greater resistance to the core cross-section. It can also be found that when the clearance is small, the core motion speed can have a more obvious effect on the damping force, but when the clearance becomes large, the change of the core motion speed almost has no effect on the damping force.

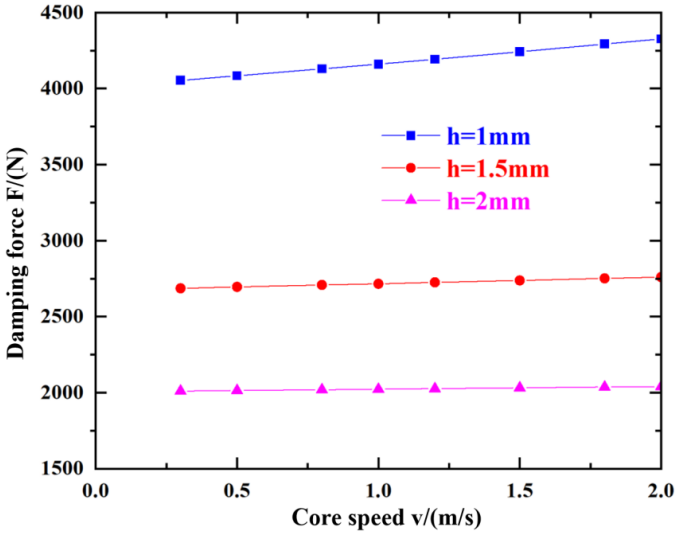

Fig.15. Relationship between damping force and core speed under different clearances

The results show that the magnetic flux density at the inlet and outlet of the flow path and the coil current becomes a linear law of change, and the damping force increases with the increase of the coil current and then decreases. In the absence of current, the damping force increases with the increase of the

speed of the core motion; after the current is passed, the damping force is very little affected by the speed of the core. Damping force with the core and cylinder cylinder clearance becomes larger and obviously reduce, and with the increase of the clearance, the core movement speed on the damping force of the influence also reduces.

CONCLUSIONS

A single-cylinder MR damper is researched in this paper, and the reasonableness of the design is verified through structural design optimization and magnetic circuit simulation, a damping force model is established, and a method of calculating the damping force of a single-cylinder MR damper is proposed, and the real damping force of the damper is obtained through the damping force test stand as the comparative data.

The results show that the magnetic flux density at the inlet and outlet of the flow channel changes linearly with the coil current, and the damping force shows an increasing and then decreasing pattern with the increase of coil current. In the absence of current, the damping force increases with the increase of the speed of the movement of the core; after the current is passed, the damping force is very little affected by the speed of the core. Damping force with the core and cylinder clearance becomes larger and significantly reduced, and with the increase of the clearance, the impact of the core speed on the damping force is also reduced. The reasonableness of the structural design and multi-objective optimization method of the single-cylinder magnetorheological damper in this paper and the correctness of the proposed damping force calculation method are verified, which provide effective theoretical support for the design of the single-cylinder MR damper in the future.

AUTHOR CONTRIBUTIONS

Na Lu had made substantial contributions to design, experimental research, data collection and result analysis; Xiaoxiao Han made critical changes to important academic content; Yan Liu made the final review and finalization of the articles to be published.

DATA AVAILABILITY

The data used to support the findings of this study are included within the article.

FUNDING STATEMENT

This article belongs to the project of the “Natural Science Research Program for Universities in Anhui Province (KJ2021ZD0144)” “Research On Structural Design Optimization And Damping Force Calculation Of Single-cylinder Magnetorheological Damper(WG25006ZD)”

CONFLICTS OF INTEREST

The authors declare that they have no conflicts of interest to report regarding the present study.

REFERENCES

Bench test method for automobile cylinder damper[S]. QC/T545-1999.

Baozhen L, Jianyong L, Wengang F, Tong X. Effects of the non-uniform magnetic field on the shear stress and the microstructure of magnetorheological fluid[J]. Journal of Magnetism and Magnetic Materials, 2021,535.

Chaoqun W, Jianglin H. Magnetic circuit analysis and optimization of magnetorheological fluid dampers[J]. Digital Manufacturing Science,2021,19(03):212-217.

Chunyuan L, Zhen P, Zhangyu R. Multi-objective optimization of NSGA-II applied to cylindrical permanent magnet linear motor[J]. Computer Age,2023, (01):21-25.

Dimension series and technical conditions for automobile cartridge damper [S]. QC/T 491-1999.

Dong K, Jiang M, Wu J. Optimization of intermittent oil recovery mechanism based on multi-objective genetic algorithm[C]. School of Mechanical Science and Engineering,Northeast Petroleum University,2023:5.

Decai L, Hongchao C, Jianwei Y, Yanjuan Z. A new modified model for the rheological properties of magnetorheological fluids based on different magnetic field[J]. Journal of Magnetism and Magnetic Materials,2020,500(C).

Feng Z, Jiang L. Structural design and magnetic field simulation of coil external magnetorheological fluid shock absorber[J]. Machine Tools and Hydraulics,2022,50(09):179-183.

Groves G W, Kazmirski K, Steed D L, et al. Solenoid actuated continuously variable shock absorber: U.S. Patent 6,464,048[P]. 2002-10-15.

Gang C, Xincai Z. Principles of electric motors and their applications[M]. Beijing:China Water Resources and Hydropower Press,2008.

Huiting B, Jun Z, Shouhu X, Xiaohui R, Xinglong G. Mechanical performance of a novel magnetorheological fluid damper based on squeeze[J]. Smart Materials and Structures,2020,29(5).

Hao X, Lei W, Weicheng W, Yiping L. Design and simulation analysis of single-cylinder inflatable magnetorheological fluid damper[J]. Agricultural Equipment and Vehicle Engineering,2020,58(09):15-19.

Hongliang Z, Pingmei M, Yingchong Z. Overview of magnetorheological fluid sealing technology[J]. Lubrication and Sealing,2021,46(06):114-125.

Hua M, Shuanglian D, Yuhan S. Finite element analysis of free vibration of intermediate support flow pipe[J]. Journal of Jinggangshan University (Natural Science Edition),2021,42(03):85-89.

Jin H, Ming L, Ping D. Study on transmission performance of magnetorheological fluid clutch driven by electrothermal shape memory alloy[J/OL]. Magnetic Materials and Devices,2022,16(09):1-6.

Lijiang W, Mingkun C, Rujian L, Qiang Y. Effect of external magnetic field on damping characteristics of magnetorheological dampers[J]. Hydraulic Pneumatic and Sealing,2022,42(01):16-22.

Liejiang W, Qingjun L, Xiaomei L, Yuanzhi H, Zengguang L. Analysis of the boundary position of the plug flow region inside the damping channel of magnetorheological fluid dampers[J]. Machine Tools and Hydraulics,2020,48(15):88-92.

Li Q. Improvement of multi-objective optimization genetic algorithm and its application in sequential charging[D]. Shandong University of Science and Technology,2020.

Munyaneza Olivier. Design and geometric parameter optimization of hybrid magnetorheological fluid damper[J]. Journal of Mechanical Science and Technology,2020,34(7):2953-2960.

Tieying G, Zhanghui Y.Simulation analysis of damping characteristics of magnetorheological fluid damper[J]. Machine Tools and Hydraulics,2018,46(09):148-150+163.

Yuanzhi H. Research on the damping force of magnetorheological fluid damper based on the flow state inside the damping channel[D]. Lanzhou University of Solenoid actuated continuously variable shock absorber: U.S.Patent 6,464,048[P].2002.10.15.

NOMENCLATURE

D the work cylinder inner diameter
D_1 the work cylinder outer diameter
L_1 the work cylinder length
h the damping clearance
D_2 the core diameter
d the piston rod diameter
l_s the effective working length of piston rod
μ the magnetorheological fluid viscosity
b the coil groove depth
L the core length
l_1 the core left side length
l_2 the length of coil slot
l_3 the core middle length
I the coil current
N the number of turns of coil at each stage
b_1 the core coil radius difference
δ the cylinder barrel thickness
r the piston rod radius
f_1 the consisting of two components
F_μ the liquid viscous damping force
F_τ the related to the magnetic field.
τ_Y the shear yield strength of MRF
μ the viscosity coefficient of the MRF
u the velocity along the flow direction
A_p the piston effective area
B the magnetic induction strength